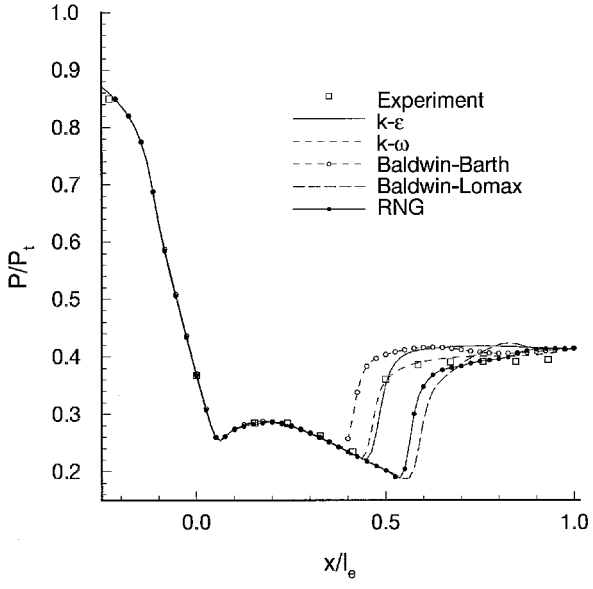

Fig. 3 Surface pressure distributions (NPR = 2.41).

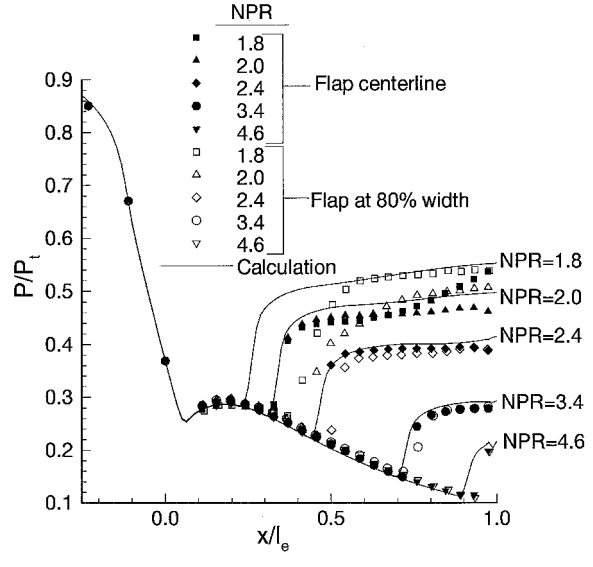

Fig. 4 Surface pressure distribution using Wilcox's k-ω turbulence model.

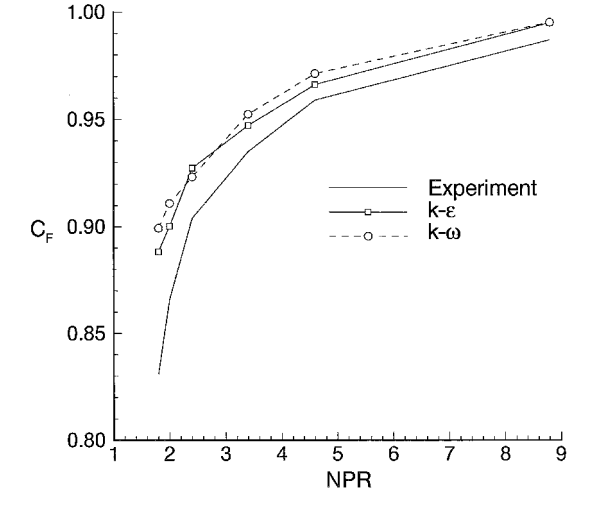

Fig. 5 Thrust coefficient predictions.

Table 1 Thrust coefficient at different pressure ratios

	NPR				
	2.0	2.4	3.4	4.6	8.8
Experiment	0.866	0.904	0.935	0.959	0.987
k-ε					
Thrust coefficient	0.900	0.927	0.947	0.966	0.995
% error in thrust	3.9%	2.5%	1.3%	0.7%	0.8%
k-ω					
Thrust coefficient	0.911	0.923	0.952	0.971	0.995
% error in thrust	5.2%	2.1%	1.8%	1.2%	0.8%

experimental results in predicting the pressure variation behind the shock. In general, the two-equation turbulence models gave the best overall agreement with the experimental results for the pressure distribution and thrust coefficient at overexpanded conditions. Figure 4 compares the computed pressure distribution over the flap using the k-ω model to the experimental results at the centerline and near the end wall at five overexpanded NPRs.

The computed thrust coefficients using the two-equation turbulence models are compared to the experimental results in Fig. 5 and Table 1. One can see that the thrust coefficient was predicted within 1.0 and 2% of the experimental values for NPRs above 50 and 30% design, respectively. At lower nozzle pressure ratios, two-dimensional flow predictions are inadequate because of the strong three-dimensional flow effects behind the shock, which are observed in the experimental results.

Acknowledgment

This work was sponsored by Ohio Aerospace Institute Subgrant 120520. The computational work was performed on the Cray Y-MP8 of the Ohio Supercomputer Center.

References

[1]Hunter, C. A., "An Experimental Analysis of Passive Shock-Boundary Layer Interaction Control for Improving the Off-Design Performance of Jet Exhaust Nozzles," M.S. Thesis, George Washington Univ., Washington, DC, Sept. 1993.

[2]Cooper, G. K., and Sirbaugh, J. R., "PARC Code: Theory and Usage," Arnold Engineering Development Center, TR-89-15, Arnold AFB, TN, Dec. 1989.

Lobed Mixers Using Simultaneous Laser-Induced Fluorescence and Mie Scattering

David M. Milam,* Mo Samimy,† and Steven Martens‡
Ohio State University, Columbus, Ohio 43210

Introduction

EFFICIENT mixing between two streams of fluids is important in many applications. The existence of large-scale

Received April 11, 1996; revision received Dec. 6, 1996; accepted for publication Jan. 2, 1997.

*Graduate Student, Department of Mechanical Engineering; currently with Caterpillar Technology Center, Mossville, IL 61552.

†Professor, Department of Mechanical Engineering. Associate Fellow AIAA.

‡Postdoctoral Fellow, Department of Mechanical Engineering; currently with General Electric Aircraft Engines, Cincinnati, OH 45215. Member AIAA.

turbulence structures in the mixing region and the entrainment of fluids from both streams into the mixing region by these structures are essential to the mixing process. It is well known that large-scale streamwise vortices can be used effectively to augment the mixing because of spanwise, normal, or ring vortices. One method of inducing large-scale streamwise vortices is the use of lobed mixers. The lobed mixer introduces an increased interface between two fluid streams along with a cross-stream velocity with alternating signs, which ultimately rolls into large-scale streamwise vortices. Many investigators have studied lobed mixers in various configurations. Over 30 references are cited in Belovich et al.[1] The study by Belovich et al.[1] in coaxial lobed mixers with inner lobed nozzles visualized the inner stream and showed the effects of a number of lobes and lobe geometry on the spreading of the inner jet (large-scale mixing between two streams), for seven different lobed nozzles at three flow conditions. This Note presents experimental results, in the same configuration used by Belovich et al.,[1] on small-scale mixing (mixing on a pixel level) between the inner and outer streams, and also additional information on the physics of the mixing processes. The results presented here are obtained by using a novel experimental technique to simultaneously visualize both the inner and outer streams.

Experimental Facility and Technique

The experiments were conducted at the Ohio State University Aeronautical and Astronautical Research Laboratory. The coaxial flow facility and nozzles investigated here are the same as were used in Belovich et al.[1] and are described in detail in Belovich[2] and Milam.[3] The three nozzles investigated include a baseline circular nozzle (nozzle B), a nozzle with a convoluted exit to increase the interfacial area without inducing streamwise vorticity (nozzle 2), and a lobed mixer nozzle with a 20-deg outward penetration angle and a 19-deg inward penetration angle to induce streamwise vorticity (nozzle 3). The nozzle designations here are consistent with those of Belovich et al.[1] All three nozzles had the same exit area of 451 $\pm$ 2 mm^2. The baseline nozzle diameter D was 25.4 mm. The outer nozzle for the coaxial flow was a 76.2-mm-diam circular nozzle.

For the results presented here, the inner flow velocity was 30 m/s, and the outer or annular flow velocity was either 10 or 30 m/s (inner-to-outer velocity ratios of 3:1 and 1:1). The 30:10 flow case was chosen to examine the effects of induced streamwise vortices in the presence of transverse ring vortices caused by Kelvin–Helmholtz instabilities. The 30:30 flow case, with a minimized transverse velocity gradient and thus, weakened convoluted ring vortices, allowed for the study of the flowfield with mixing dominated by streamwise vorticity.

The method for obtaining simultaneous flow visualizations for these experiments was a combination of two imaging techniques. This novel approach obtains separate but simultaneous images of each of the two streams forming the coaxial jet. The technique used for the outer flow was planar laser-induced fluorescence (PLIF) using acetone, and the technique used for the inner flow was Mie scattering from oil droplets. Laser light was provided by the fourth harmonic (λ = 266 nm) of a Quanta-Ray GCR-4, Nd:YAG laser. The laser beam was spread into a planar sheet of light using appropriate optics. The simultaneous capturing of signals from each stream was facilitated by the use of these two different laser diagnostic techniques that yielded different wavelength signals for the same interrogating laser wavelength. The fluorescence signal in the outer stream occurred at wavelengths between 350–550 nm. The Mie scattering signal from the inner flow was at the input wavelength of 266 nm with no detectable fluorescence from the oil droplets.

Using two synchronized Princeton Instruments 14-bit cameras, 100 images were obtained for each stream during a single experimental run. The first camera was equipped with a Nikon uv lens, capable of detection in both the uv and the visible range. The signal from the Mie scattering of the uv light was detected by this camera. The fluorescence signal that occurred in the visible range was blocked from this camera with a narrow bandpass filter with a half-width of 10 nm centered at 266 nm. The signal from the fluorescence was detected by the second camera that utilized a Tamron lens for visible light collection. This lens was equipped with a simple color filter to ensure blockage of the uv light.

Experimental Results and Discussion

Figure 1 shows typical instantaneous streamwise images of the inner and outer streams for the lobed mixer and the 30:10 flow case. The inner flow image corresponds to the Mie scattering from oil droplets in the flow, and the outer flow image corresponds to fluorescence from acetone vapor in the flow. These images show streamwise views of the flowfield with the laser sheet passing from crest to crest of lobes of the lobed mixer. The dark region seen in the center of the image (Fig. 1b) extending from x/D = 0 to 3 is the central core of the inner jet that is approximately 2.5 times shorter than that of the baseline nozzle case (not shown here). While simultaneous flow visualization images such as those shown in Fig. 1 provide a qualitative understanding of flow structure and mixing process, more quantitative information can be obtained by examining the 14-bit images stored in a 288 by 192 intensity array. This type of information is beneficial for illustrating relative differences between different lobe nozzle designs.

Figure 2 shows average inner stream images (calculated from 100 instantaneous images) for a laser sheet passing from the trough of one lobe to the trough of the lobe located 180 deg away from it for nozzles 2 and 3. Figure 2a shows a gradual growth of the inner flow for nozzle 2 (the nozzle with the same interfacial area as nozzle 3, but with little induced streamwise vorticity). Figure 2b, however, shows that a different mechanism is responsible for the mixing between the lobes for nozzle 3. Rather than a gradual growth as seen in Fig. 2a, there is a sudden jump in the jet spread around x/D = 1.5. This phenomenon will be explained next by examining the entrainment of inner flow into the regions between adjacent lobes by streamwise vortices.

Figure 3a shows the normalized intensities in a radial direction from the centerline of nozzle 2 through the region between two adjacent lobes, for a number of streamwise locations. The intensities are normalized by the intensity at the centerline that

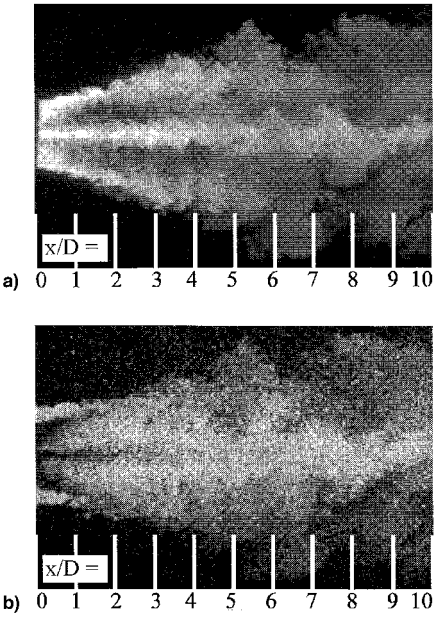

Fig. 1 Nozzle 3 streamwise images, 30:10 flow case. Instantaneous a) inner and b) outer flows.

is the highest intensity value in each radial cut. As the jet propagates downstream, the intensity levels gradually increase in the outwardly radial direction. This is caused by the mixing between two streams because of the convoluted ring vortices. Similar plots for nozzle 3 (Fig. 3b) show a hump in the intensities as the region is traversed from the centerline outward through the region between two adjacent lobes. This hump is indicative of the radial distance between the lobes where counter-rotating streamwise vortices from adjacent lobes begin to interact. This interaction between two adjacent vortices becomes noticeable at $x/D = 1.5$. A similar phenomenon was also observed by McCormick and Bennett[4] in two-dimensional lobed mixers, which they called pinch-off of the normal vortex by streamwise vortices.

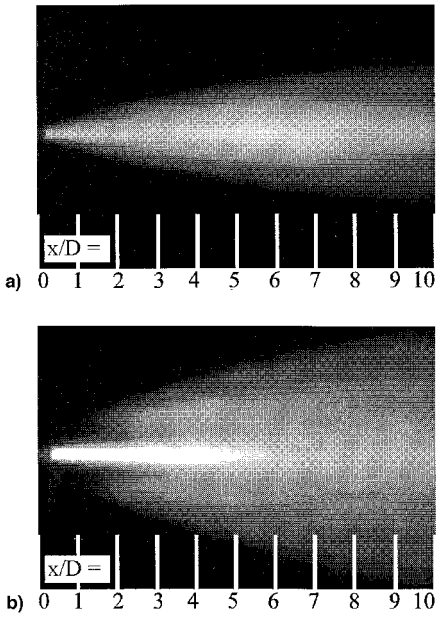

Fig. 2 Nozzles a) 2 and b) 3 streamwise trough-to-trough images.

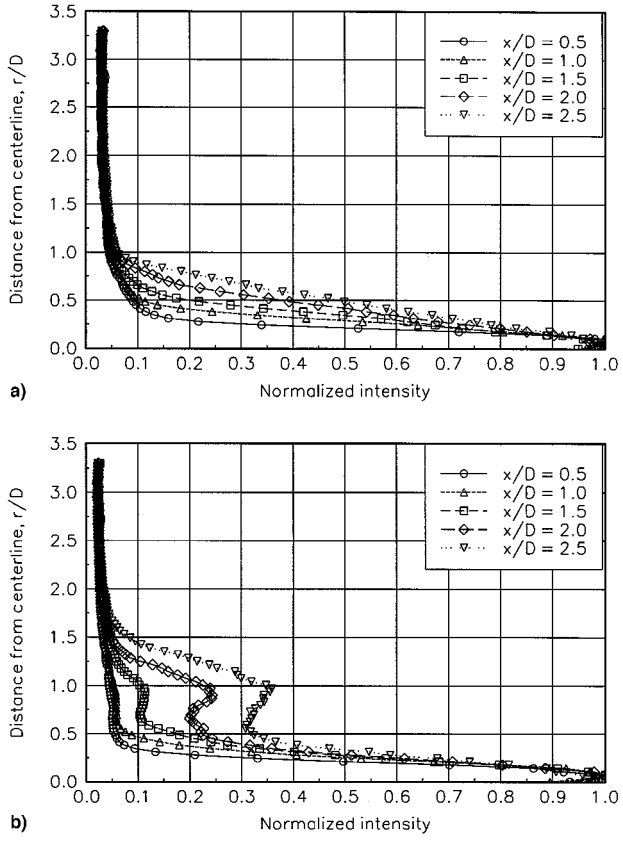

Fig. 3 Intensity values for the trough-to-trough cuts, nozzles a) 2 and b) 3.

Belovich et al.[1] and Belovich[2] used visualization of the inner jet to explore large-scale mixing characteristics of lobed mixers. While this kind of information is very useful in applications such as mixing of the core flow and bypass flow in a gas turbine, information on small-scale mixing is crucial in applications such as combustors. In the present work, simultaneous imaging of both streams were used to obtain small-scale mixing (mixing on a pixel level) between two streams. A pixel is an image of a volume of the flowfield with approximately 0.6 $\times$ 0.6 $\times$ 0.5 mm^3 dimensions. This was accomplished by choosing a signal threshold level in the inner and outer stream cross-sectional images, signifying the presence or absence of fluid from that stream and then finding regions where the signal from both streams is present (mixing on a pixel level). This is done by looking at a histogram of the intensities in the images. The intensity value for each pixel with an intensity below the threshold level was set to zero (corresponding to no fluid) or one for pixels with an intensity above the threshold level (corresponding to the existence of fluid), for both the inner and outer stream images. The matrices of intensities were added and the pixel locations that had a value of 2 were counted as a mixed region (both fluids present). The basis for this is that if a pixel records a signal from both the inner and outer flow, the fluids have been exposed to each other and have mixed at a pixel level. Belovich et al.[1] used a similar image thresholding technique to look at the overall inner flow growth since they did not visualize the outer flow. In the present study, using the technique of simultaneous Mie scattering and fluorescence, both inner and outer flow images were collected, allowing for a determination of the mixing between two streams.

Figure 4 shows a plot of the mixed region (small-scale mixing) vs axial position for the 30:10 and the 30:30 flow case for all three nozzles. Nozzle 2 has approximately the same mixed region growth rate as the baseline nozzle. This suggests that the increase in the mixed region for nozzle 2 compared to the baseline nozzle is through the same mechanism. Nozzle 3 shows that the streamwise vorticity produces a significantly higher mixing growth rate (approximately four times higher for $x/D > 3$), compared to nozzles 2 and B. The relative trends for the growth of the mixed region shown in Fig. 4 are similar to the growth of the inner jet examined by Belovich et al.[1] However, the results presented here are a more direct measure of the performance of lobed mixers in terms of small-scale mixing, which is important in applications such as combustors. The results presented here confirm the findings of Manning[5] on the effectiveness of lobed mixers obtained using water-tunnel experiments. The mixing growth rates for 30:30 and 30:10 were almost the same. This suggests that streamwise

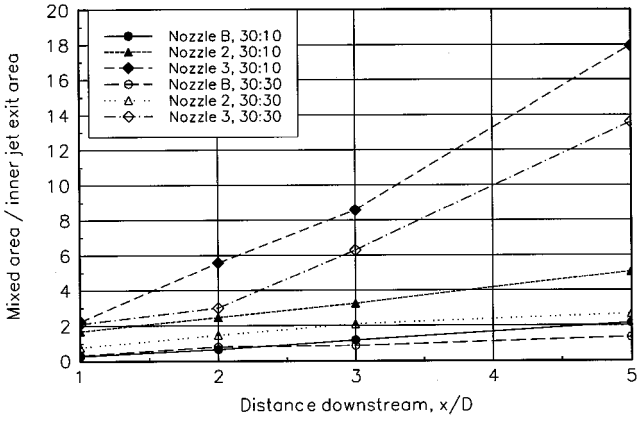

Fig. 4 Growth of mixed region for the 30:10 and 30:30 flow case.

vortices generated by lobed mixers are much more effective than ring vortices in providing entrainment and mixing.

Acknowledgments

This project was partially funded by the Air Force Office of Scientific Research with W. M. Roquemore as Contract Monitor. S. Martens is appreciative for support through a postdoctoral fellowship from the Ohio State University. The authors thank P. S. Clancy, J.-H. Kim, and V. M. Belovich for their assistance in performing the experiments.

References

[1]Belovich, V. M., Samimy, M., and Reeder, M. F., "Dual Stream Axisymmetric Mixing in the Presence of Axial Vorticity," *Journal of Propulsion and Power*, Vol. 12, No. 1, 1996, pp. 178–185.

[2]Belovich, V. M., "Mixing Processes in a Coaxial Geometry with a Central Lobed Mixer Nozzle," Ph.D. Dissertation, Ohio State Univ., Columbus, OH, 1995.

[3]Milam, D. M., "An Investigation of Coaxial Jet Mixing with Axial Vorticity Using Simultaneous LIF and Mie Scattering," M.S. Thesis, Ohio State Univ., Columbus, OH, 1996.

[4]McCormick, D. C., and Bennett, J. C., Jr., "Vortical and Turbulent Structure of a Lobed Mixer Free Shear Layer," AIAA Paper 93-0219, Jan. 1993.

[5]Manning, T. A., "Experimental Studies of Mixing Flows with Streamwise Vorticity," M.S. Thesis, Massachusetts Inst. of Technology, Cambridge, MA, 1991.

Combustion and Microexplosion of Han-Based Liquid Gun Propellants at Elevated Pressures

C. Call*
University of California, Davis, California 95616
D. L. Zhu† and C. K. Law‡
Princeton University, Princeton, New Jersey 08544
and
S. C. Deevi§
Philip Morris, Richmond, Virginia 23234

Introduction

PRESENTLY there exists much interest in the use of a class of liquid propellants (LP) for the launching of gun ordnance.[1] These propellants are composed of salts of hydroxylammonium nitrate (HAN) and an aliphatic ammonium nitrate (AAN) dissolved in water. Since HAN is oxygen rich based on N_2–H_2O stoichiometry, whereas AAN is oxygen deficient, they are usually mixed in stoichiometric proportions for maximum propellant energy density. The AAN that is being widely studied at present is triethanolammonium nitrate (TEAN); the specific LP being tested is coded 1845, which consists of 63.2% HAN, 20% TEAN, and 16.8% water, all by weight. This LP has a heating value of about 1 kJ/g and a calculated adiabatic flame temperature of 2285 K. This is the LP adopted for most of the tests conducted in the present study.

Received July 4, 1996; revision received Dec. 15, 1996; accepted for publication Dec. 30, 1996.

*Graduate Student, Department of Mechanical Engineering.

†Technical Staff, Department of Mechanical and Aerospace Engineering.

‡Robert H. Goddard Professor, Department of Mechanical and Aerospace Engineering. Fellow AIAA.

§Research Scientist, Research Center.

Very little is known about the combustion properties of these propellants, although some useful information has been recently reported.[2–4] Specifically, in Ref. 2 it was determined, for atmospheric pressure conditions, that the liquid-phase reaction of LP-1945 is initiated around 200–230°C, that HAN is the component that initiates this reaction, that in practical situations this temperature range can be lower because of the preferential gasification of water and thereby concentration of the salts prior to the onset of reaction, and that there seems to exist a critical salt concentration at which reaction occurs spontaneously. In Ref. 3 data on supported droplets in very high-pressure environments were reported, including observations of droplet microexplosion. In Ref. 4 the flame propagation process within the LP was studied under high-pressure situations, from 68 to 300 atm. The results again demonstrate that it is HAN that initiates the reaction. In Ref. 5 the thermodynamic critical parameters of the LP were estimated. The results show that the critical pressure can be very high such that the LP may not attain criticality during most of the burning time within the ultrahigh pressure environment of the gun chamber.

In the present investigation we extend the droplet combustion work of Ref. 2 to mildly elevated pressure environments. The work is primarily motivated by the recognition that liquid-phase reaction is a crucial element of LP combustion, and that its initiation and intensity can be greatly affected by the liquid temperature. Because thermodynamically the attainable liquid temperature increases with increasing pressure, it is reasonable to expect that the liquid-phase reaction can be correspondingly facilitated by increasing the system pressure. We shall demonstrate subsequently that this concept of pressure-enhancement is indeed viable.

The experimental methodology is presented in the next section, which is followed by discussion of the experimental results.

Experimental Methodology

A steady-flow combustion chamber is used to study the gasification and microexplosion of freely falling LP droplets. A schematic of the apparatus as well as details of the experimentation can be found in Refs. 6 and 7. The experiment involves injecting downward a steady stream of monodisperse and equally spaced LP droplets into the hot postcombustion zone of a flat flame, and observing the subsequent combustion event by freezing the droplet image with stroboscopic backlighting. A solid-state charge-coupled device camera is mounted on a zoom microscope for droplet imaging. The camera signal is transmitted to a video recorder and a high-resolution monitor, allowing a convenient means for focusing and recording. The overall magnification from the actual droplet size to the video monitor is about $\times 275$, and the measurement uncertainty is less than 2% of a typical 200-μm droplet. All of the steady droplet gasification data were taken with a temperature variation of less than 50 K; in most cases the variation is less than 25 K. The gas temperature reported in the following is the thermocouple measured value at about the midpoint in the droplet lifetime. Typical accuracies of experiments of this nature are discussed in Ref. 6.

Results and Discussions

Observationally, there are several qualitative features of HAN-based LP combustion that distinguish it from hydrocarbon fuels. First, hydrocarbon fuels have a thin blue diffusion flame that surrounds the droplet stream. This diffusion flame can also be accompanied by a yellow soot layer that is interior to it. The flame standoff ratio typically ranges from 4 to 10. However, for LP combustion, the droplet stream is completely surrounded by a faint orange glow that extends out up to 40 droplet radii. Thus, in contrast to hydrocarbon fuels, there is no clear distinction between pure vaporization and thin flame burning. The gasification rates of these propellants are low, primarily controlled by that of water, as will be shown later.